

# Universality of Osmotic Equation of State in Star Polymer Solutions

Takashi Yasuda,<sup>1</sup> Masanobu Ino,<sup>1</sup> Takamasa Sakai,<sup>1,\*</sup> and Naoyuki Sakumichi<sup>1,†</sup>

<sup>1</sup>*Graduate School of Engineering, The University of Tokyo, 7-3-1 Hongo, Bunkyo-ku, Tokyo, Japan.*  
(Dated: February 28, 2023)

We experimentally measure the osmotic pressures of linear polymers and three-, four-, and eight-arm star polymers in a good solvent via membrane osmometry. These results reveal that the osmotic equations of state in the star polymer solutions are universally described by the same scaling function that describes linear polymer solutions. This universality is achieved by canceling increasing overlap concentrations and decreasing osmotic pressure, owing to the increased arm number. We further clarify the molar mass and arm number dependencies of the gyration radius and interpenetration factor, ensuring universality in star polymer solutions.

Star polymers consisting of several linear chains radiating from a central core have attracted considerable attention in recent decades for numerous applications in life sciences and nanotechnology [1–3]. Recently, the value of the use of “semidilute” star polymer solutions, where polymers overlap, has increased. This is because gels with a precisely controlled polymer network [4] can be synthesized by end-linking star polymers in a semidilute regime; that is, the polymer concentration  $c$  exceeds the overlap concentration  $c^*$ . Chemical gels [5–8] and physical gels [9–14] consisting of precisely controlled permanent and transient networks, respectively, have been fabricated, with their reproducibility and controllability leading to significant advances in polymer physics [15–20].

Although providing insights into semidilute star polymer solutions ( $c > c^*$ ) is becoming increasingly important, the physical understanding is limited. For example, the governing law of their osmotic pressure  $\Pi$ , one of the most fundamental physical properties, remains unclear despite pioneering efforts [21–26]. The major difficulty is that reliable measurement (through membrane osmometry) of  $\Pi$  of semidilute star polymer solutions is reported only for three-arm star polymers [21]. This situation is in contrast to dilute star polymer solutions ( $c < c^*$ ); the gyration radius and second virial coefficient have been extensively investigated via light scattering [27–47].

Before considering star polymers, we briefly review  $\Pi$  of (electrically neutral) flexible linear polymer solutions. Numerous theoretical [48–52] and experimental [21, 53–55] studies have clarified that  $\Pi$  of dilute and semidilute linear polymers in good solvents is *universally* described by the following osmotic equation of state (EOS):

$$\hat{\Pi} = f_{\Pi}(\hat{c}), \quad (1)$$

where  $\hat{\Pi} \equiv \Pi M / (cRT)$  is the reduced osmotic pressure and  $\hat{c} \equiv c/c^*$  is the reduced polymer mass concentration  $c$  normalized by overlap concentration  $c^* \equiv 1/(A_2M)$ . Here,  $M$ ,  $R$ ,  $T$ , and  $A_2$  are the molar mass, gas constant,

absolute temperature, and second virial coefficient, respectively. Figure 1(a) demonstrates that different types of linear polymer solutions (open triangles) converge to Eq. (1) (black solid curves) [21, 53]. In the dilute regime ( $0 \leq \hat{c} < 1$ ), each polymer chain is isolated, and  $\Pi$  is described through the virial expansion [56]:

$$\hat{\Pi} = 1 + \hat{c} + \gamma \hat{c}^2 + \dots, \quad (2)$$

where  $\gamma \approx 0.25$  is the dimensionless virial ratio of the third virial coefficient [57]. In the semidilute regime ( $\hat{c} > 1$ ), the polymer chains overlap without isolation, and  $\Pi$  is independent of  $M$ . Consequently, Eq. (1) is asymptotic to the following scaling law [black dashed line in Fig. 1(a)] [48, 49]:

$$\hat{\Pi} = K \hat{c}^{\frac{1}{3\nu-1}}, \quad (3)$$

where  $K \approx 1.1$  and  $1/(3\nu - 1) \approx 1.31$ . Here,  $\nu \approx 0.588$  is the excluded volume parameter for good solvents [56] and is known as the universal critical exponent of the self-avoiding-walk universality class [58].

In this Letter, we investigate the universal law of  $\Pi$  in star polymer solutions with up to eight arms. We experimentally measure  $\Pi$  via membrane osmometry and find that  $\Pi$  depends on the number of arms  $f$  but not on the molar mass  $M$  in the semidilute regime ( $c > c^*$ ). Furthermore, we find that the dimensionless  $\hat{\Pi}$  of star polymer solutions is described by the same EOS as the linear polymer solutions [Eq. (1)] in the dilute and semidilute regimes. Figure 1 demonstrates that the linear, three-arm, four-arm, and eight-arm star polymer solutions agree with Eq. (1) (black solid curve). The difference between the linear ( $f = 2$ ) and star ( $f \geq 3$ ) polymer solutions manifests as increasing  $c^*$  and decreasing  $\Pi$ , owing to increased  $f$ . Furthermore, we clarify  $M$  and  $f$  dependences of the gyration radius  $R_g$  ( $\propto M^\nu$ ) and interpenetration factor  $\Psi^*$ , ensuring the universality of EOS in star polymer solutions.

*Materials and methods.* — We used linear, three-arm, four-arm, and eight-arm star PEG with  $M = 20$  kg/mol (Polyethylene glycol 20000, Sigma-Aldrich),  $M = 20$  kg/mol (SUNBRIGHT GL2-200MA, NOF Co., Japan),  $M = 10$  and 40 kg/mol (SUNBRIGHT PTE-100MA

\* Corresponding author: sakai@gel.t.u-tokyo.ac.jp

† Corresponding author: sakumichi@gel.t.u-tokyo.ac.jp

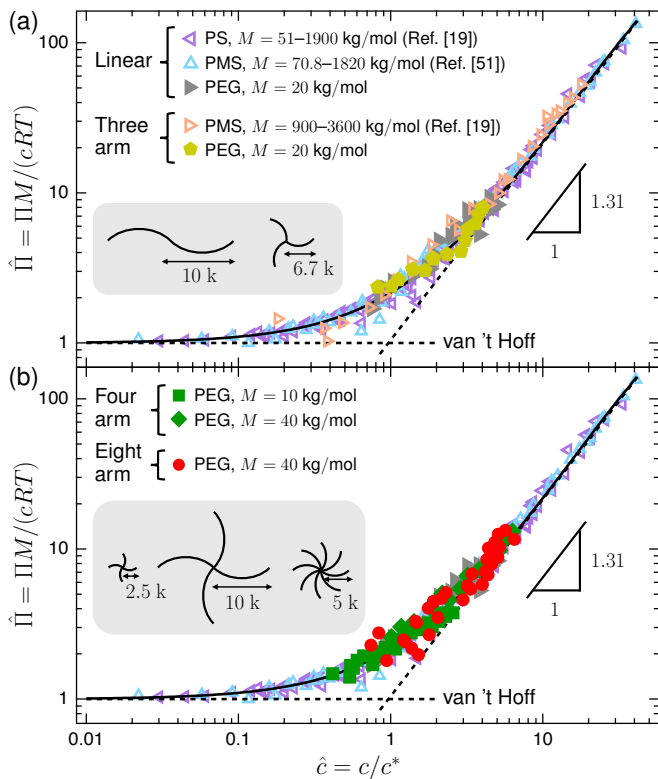


FIG. 1. Universality of osmotic EOS in linear and star polymers in good solvents. The open triangles represent two kinds of linear polymers [poly( $\alpha$ -methylstyrene) (PMS) with  $M = 70.8$ – $1820$  kg/mol [53] and poly(styrene) (PS) with  $M = 51$ – $1900$  kg/mol [21] in toluene solutions. The open stars represent the three-arm star polymers [PMS with  $M = 900$ – $3600$  kg/mol [21] in toluene solutions. The gray-filled triangles represent the linear polymers [poly(ethylene glycol) (PEG) with  $M = 20$  kg/mol] in aqueous solutions. The yellow pentagons, green squares and diamonds, and red circles represent the star PEG in aqueous solutions for (a) three arms with  $M = 20$  kg/mol, (b) four arms with  $M = 10$  and  $40$  kg/mol and eight arms with  $M = 40$  kg/mol, respectively. We reported the data for four arms in Ref. [59]. All data collapse onto the universal EOS given by Eq. (1) (black solid curve), which is asymptotic to the van 't Hoff law ( $\hat{\Pi} = 1$ ) as  $\hat{c} \rightarrow 0$  and the scaling law in Eq. (3) as  $\hat{c} \rightarrow \infty$  (black dashed lines).

and 400MA, NOF Co., Japan), and  $M = 40$  kg/mol (8-arm PEG-OH(TP), XIAMEN SINOPEG BIOTECH Co., Ltd., China), respectively. We confirmed that the effect of the difference in end-functional groups on osmotic pressure is negligible [Supplemental Material (SM), Sec. S1]. We prepared samples for the initial polymer mass concentrations  $c_0 = 20$ – $160$  g/L in aqueous solutions at 298 K. Here, we define the polymer mass concentration as the polymer weight divided by the solvent volume, rather than the solution volume, to extend the universality of EOS to higher concentrations (see SM, Sec. S1 in Ref. [59]).

We measured  $\Pi$  of the linear and star polymer solu-

tions using membrane osmometry. We used controlled aqueous poly(vinylpyrrolidone) (PVP, K90, Sigma-Aldrich) solutions at  $T = 298$  K, whose concentration dependence of osmotic pressure  $\Pi_{\text{ext}}$  was reported as  $\Pi_{\text{ext}} = 21.27c_{\text{ext}} + 1.63c_{\text{ext}}^2 + 0.0166c_{\text{ext}}^3$  for  $c_{\text{ext}} \leq 200$  g/L [60]. Here, the PVP concentration  $c_{\text{ext}}$  is defined as the polymer weight divided by the solution volume. As shown in the schematic in Fig. 2(a), each solution sample was placed in a microdialyzer (MD300, Scienova) with a semipermeable membrane (mesh size, 3.5 kDa). Each microdialyzer was immersed in an aqueous polymer (PVP) solution at a certain concentration  $c_{\text{ext}}$  with stirring. Subsequently, each system reached equilibrium at  $\Pi = \Pi_{\text{ext}}$ . (Reaching equilibrium was ensured. See SM, Sec. S3.) Each solution sample was changed in weight ( $W_0 \rightarrow W$ ) and polymer mass concentration ( $c_0 \rightarrow c$ ) from the as-prepared state to equilibrium. For each sample, we tuned  $c_{\text{ext}}$  to satisfy  $W/W_0 \approx 1$ . We calculated  $c$  as  $c = c_0/[W/W_0 + (W/W_0 - 1)c_0/\rho_s]$ , where  $\rho_s$  is the density of solvents, using  $\rho_{\text{water}} \approx 1.0 \times 10^3$  kg/m<sup>3</sup> for aqueous solvents. All experimental results for  $\Pi$  are available in SM, Sec. S3.

*Results.*— Figure 2(b) presents a comparison of the  $c$  dependence of  $\Pi$  for different arm numbers ( $f$ ), demonstrating that  $\Pi$  decreases with increasing  $f$  when  $M$  is constant. To compare the samples of different  $f$  at fixed  $M$ , we disregarded the polydispersity ( $\leq 1.2$ ) of each sample and slight differences in the average molar mass with different  $f$  due to synthesis inaccuracies. For a low  $c$  (dilute regime),  $\Pi$  follows  $\Pi = cRT/M$  (van 't Hoff law), which is independent of  $f$ . By contrast, for a high  $c$  (semidilute regime),  $\Pi$  decreases with increasing  $f$  (red and yellow arrows) at fixed  $c$  and  $M$ . The decrease in  $\Pi$  among  $f = 4$  and  $8$  (red arrow) is significant, whereas only minor differences arise between  $f = 2$  and  $3$  (yellow arrow). Consequently, the decrease in  $\Pi$  was not recognized in Ref. [21] examining  $f = 2$  and  $3$ . This decrease in  $\Pi$  owing to branching cannot be explained by the conventional scaling argument [described before Eq. (3)] for semidilute linear polymer solutions; the origin of this decrease is discussed below.

Figure 2(c) shows the  $c$  dependence of  $\Pi$  with different  $M$  for four-arm star polymer solutions, which are asymptotic to an  $M$ -independent scaling law in the semidilute regime ( $c \gg c^*$ ). The star polymer solutions exhibit the  $M$ -independent scaling law in the semidilute regime, showing the same characteristics as linear polymer solutions [Eq. (3)] [48, 49]. The exponent of the scaling law  $3\nu/(3\nu - 1) \approx 2.31$  is independent of  $f$ , whereas the prefactor of  $\Pi$  depends on  $f$ .

We show that  $c^*$  at fixed  $M$  increases as  $f$  increases by evaluating  $c^*$  from the square-root plots [56] of the experimental results shown in Fig. 2(b) and (c). From the virial expansion in Eq. (2), we have  $\hat{\Pi} = [1 + \hat{c}/2 + (\gamma - 1/4)\hat{c}^2/2]^2 + O(\hat{c}^3)$ . Together with  $\gamma \approx 1/4$  for star polymer solutions with few arms (SM,

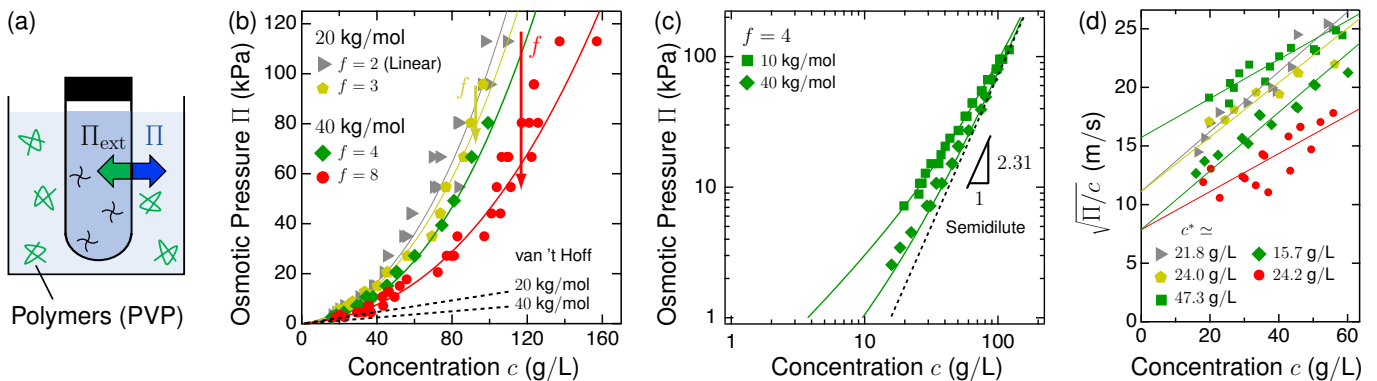


FIG. 2. Osmotic pressure  $\Pi$  of aqueous solutions with the linear and star PEG. (a) Membrane osmometry with a microdialyzer in external aqueous polymer (PVP) solutions. We can determine  $\Pi$ , using  $\Pi = \Pi_{\text{ext}}$  at equilibrium. (b) Dependence of  $\Pi$  on polymer mass concentration  $c$  for arm numbers  $f = 2$  (linear, gray triangles) and  $f = 3$  (yellow pentagons) with the molar mass  $M = 20$  kg/mol, and  $f = 4$  (green diamonds) and  $f = 8$  (red circles) with  $M = 40$  kg/mol. In the dilute limit ( $c \rightarrow 0$ ),  $\Pi$  follows the van 't Hoff law,  $\Pi = cRT/M$  (black dashed lines). (c) Dependence of  $\Pi$  on  $c$  with  $M = 10$  and  $40$  kg/mol for  $f = 4$ . In the semidilute regime ( $c > c^*$ ),  $\Pi$  is asymptotic to the semidilute scaling law given by Eq. (3) with the exponent  $3\nu/(3\nu - 1) \approx 2.31$  (black dashed line). (d) Square-root plot of the osmotic pressure. Each solid line is a least-square fit to Eq. (4), where the fit parameter is  $c^*$ . In (b) and (c), each solid curve represents the universal EOS given by Eq. (1), using  $c^*$  evaluated in (d) with each  $M$ .

Sec. S4), we have

$$\sqrt{\frac{\Pi}{c}} \simeq \sqrt{\frac{RT}{M}} \left(1 + \frac{c}{2c^*}\right) \quad (4)$$

for a small  $c/c^*$ . Thus,  $c^*$  for each sample can be estimated by the slopes of the best-fit lines in Fig. 2(d). We obtained  $c^* = 21.8(7)$  g/L for  $f = 2$  with  $M = 20$  kg/mol;  $c^* = 24.0(10)$  g/L for  $f = 3$  with  $M = 20$  kg/mol;  $c^* = 47.3(21)$  and  $15.7(4)$  g/L for  $f = 4$  with  $M = 10$  and  $40$  kg/mol, respectively; and  $c^* = 24.2(13)$  g/L for  $f = 8$  with  $M = 40$  kg/mol. Values in parentheses represent standard errors. The obtained  $c^*$  increases as  $f$  increases at fixed  $M$ .

We validate that the obtained  $c^* \equiv 1/(A_2M) \approx 21.8$  g/L for the linear PEG in aqueous solution is consistent with the gyration radius  $R_g$  measured via light scattering in Ref. [61]. We use the following relation:

$$c^* = \frac{M}{4\pi^{3/2}R_g^3N_A\Psi^*}, \quad (5)$$

where  $N_A$  is the Avogadro constant and  $\Psi^*$  is the interpenetration factor. Because  $\Psi^* \approx 0.24$  for linear polymers [33–35, 38–42], we obtain  $R_g = [M/(4\pi^{3/2}N_A\Psi^*c^*)]^{1/3} = 6.58(7)$  nm for  $c^* = 21.8(7)$  g/L. The samples of  $M = 10$ – $40$  kg/mol used in this study correspond to polymerization degrees  $N \approx 227$ – $909$ , which are sufficiently large as  $\Psi^*$  remains constant [31, 32]. Figure 3(a) shows that  $R_g$  reported in Ref. [61] and  $R_g$  measured in this study agree with the scaling law  $R_g \propto M^\nu$  (solid line), with  $\nu \approx 0.588$  [58]. This result validates  $c^*$  determined in our analysis.

Using  $\Pi$  shown in Fig. 2(b) and (c) and  $c^*$  evaluated in Fig. 2(d), we demonstrate that the osmotic EOS in star

polymer solutions with up to eight arms is universally described by Eq. (1). We rescaled the state variables from dimensional ( $c$  and  $\Pi$ ) to dimensionless ( $\hat{c}$  and  $\hat{\Pi}$ ) for each sample and yielded the filled symbols shown in Fig. 1. The open symbols for linear and three-arm polymers in Fig. 1 were obtained by reanalyzing the reported data [21, 53] in the same manner, using  $c^* \equiv 1/(A_2M)$ . All symbols, including linear, three-arm, four-arm, and eight-arm polymers with various  $M$ , demonstrate the universality of the osmotic EOS given by Eq. (1) [21, 53]. This universality originates from canceling the decrease in  $\Pi$  [Fig. 2(b)] and the increase in  $c^*$  [Fig. 2(d)] as  $f$  increases.

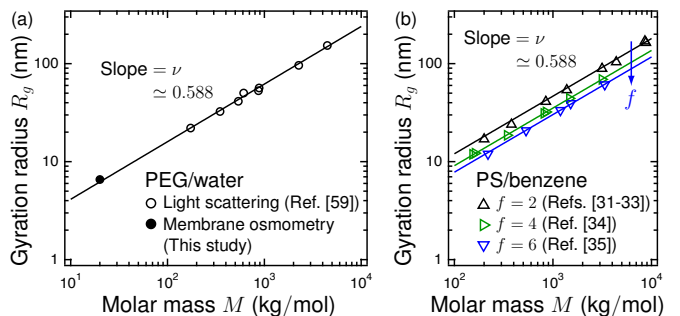


FIG. 3. Molar mass ( $M$ ) dependence of gyration radius  $R_g$  at 298 K for (a) linear PEG in aqueous solutions and (b) linear (black upward triangles), four-arm (green rightward triangles), and six-arm (blue downward triangles) poly(styrene) in benzene solutions. Each solid line represents  $R_g \sim M^\nu$  with  $\nu \approx 0.588$ . In (a), the results measured via membrane osmometry (filled circle) are consistent with those measured via light scattering [61] (open circles). In (b), the data are taken from Refs. [33–37], measured via light scattering.

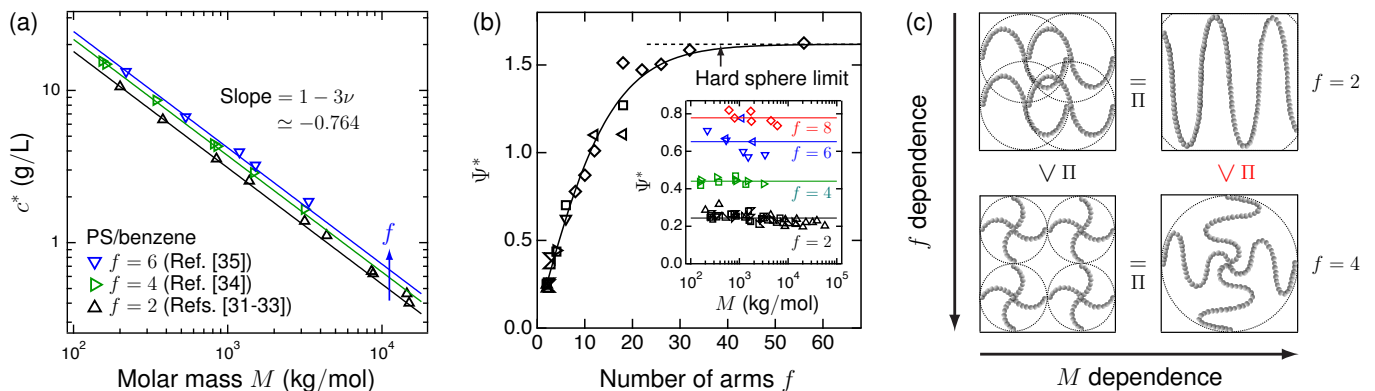


FIG. 4. (a) Molar mass dependence of  $c^*$  for the linear (black upward triangles), four-arm (green rightward triangles), and six-arm (blue downward triangles) poly(styrene) in benzene solutions at 298 K. (b) Interpenetration factor  $\Psi^*$  for various  $f$ . The error bars indicate the standard deviation. For large  $f$ ,  $\Psi^*$  is asymptotic to the hard-sphere value  $\Psi^* \approx 1.61$  (dashed line) [62]. Inset: Molar mass dependence of  $\Psi^*$  for  $f = 2$  (black symbols),  $f = 4$  (green symbols),  $f = 6$  (blue symbols), and  $f = 8$  (red symbols) with various polymers and solvents at different temperatures. Here, different symbols indicate differences in the references. The data in (a) and (b) are taken from Refs. [33–37] and Refs. [33–47], respectively, measured via light scattering. (c) Schematic of the  $M$  and  $f$  dependencies of  $\Pi$  in the semidilute linear and star polymer solutions at fixed  $c$ .

We emphasize that the  $A_2$ -based definition of the overlap concentration,  $c^* \equiv 1/(A_2M)$ , is essential in exhibiting the universality of osmotic EOS in star polymer solutions. The commonly used  $R_g$ -based definition of the overlap concentration is  $c_g^* \equiv 3M/(4\pi N_A R_g^3)$ , where the polymer chains begin to overlap to fill the space. However,  $c/c_g^*$  is not the universal scaling parameter for star polymers, because  $c_g^*/c^* = 3\sqrt{\pi}\Psi^*$  includes the interpenetration factor  $\Psi^*$ . Here,  $\Psi^*$  depends on  $f$  due to the high segment density near the central core preventing polymer chain penetration. In Ref. [21], the universality of the osmotic EOS was not revealed because  $c/c_g^*$  was used to compare  $f = 2$  and  $f = 3$ .

*Discussion.*— To ensure the universality of Eq. (1) (i.e., the function  $f_{\Pi}$ ) for various polymers and solvents, we investigated  $M$  and  $f$  dependencies of (i)  $c^*$  and (ii)  $\Pi$ . Figure 2(d) and (b) experimentally show (i) and (ii), respectively, for PEG in aqueous solutions;  $c^*$  is an increasing sequence of  $f$ , and  $\Pi$  is a decreasing sequence of  $f$ .

Regarding (i), using the data reported in Refs. [33–37], Figs. 3(b) and 4(a) show that  $f$ -arm star poly(styrene) in benzene solutions exhibits the scaling law  $R_g \propto M^\nu$  and  $c^* \propto M^{1-3\nu}$ , respectively. Here, the latter scaling law comes from Eq. (5) with the fact that  $\Psi^*$  is independent of  $M$  (see below):  $c^* \propto MR_g^{-3} \propto M^{1-3\nu}$ . Moreover, Figs. 3(b) and 4(a) show that  $R_g$  and  $c^*$  are decreasing and increasing sequences of  $f$  at fixed  $M$ , respectively (blue arrows); this is because each arm length is proportional to  $M/f$ .

Organizing the data of  $R_g$  and  $A_2$  obtained from Refs. [33–47], Fig. 4(b) shows that  $\Psi^*$  is an increasing sequence of  $f$  from  $\Psi^* \approx 0.24$  for  $f = 2$  (linear polymer [33–35, 38–42]) to  $\Psi^* = 20\sqrt{5}/(3^{5/2}\sqrt{\pi}) \approx 1.61859$  (hard-sphere value [40, 62]) for  $f \rightarrow \infty$ , where the

polymer chains can be regarded as noninterpenetrating spheres. Because  $c^* \propto 1/(R_g^3\Psi^*)$  is an increasing sequence of  $f$ , the decrease in  $R_g^3$  is more dominant than the increase in  $\Psi^*$  as  $f$  increases. The inset in Fig. 4(b) demonstrates that  $\Psi^*$  is a universal parameter depending only on  $f$ ;  $\Psi^*$  is independent of  $M$ ,  $T$ , and the kind of polymer and solvent, at each  $f$ , by using four polymer-solvent systems [poly(styrene)/benzene, poly(styrene)/toluene, poly(butadiene)/cyclohexane, and poly(isoprene)/cyclohexane] at various  $M$  and  $T$  [33–42, 45, 46]. (Detailed references are provided in SM, Sec. S5.)

Regarding (ii), we investigate  $M$  and  $f$  dependencies of  $\Pi$  in the semidilute regime ( $c \gg c^*$ ). Equation (3) can be rewritten as

$$\Pi = \frac{KRT}{Mc^*} c^{\frac{3\nu}{3\nu-1}}. \quad (6)$$

Because  $c^* \propto M^{1-3\nu}$  for any  $f$  [Fig. 4(a)], Eq. (6) indicates that  $\Pi$  is independent of  $M$  not only for linear polymers but also for star polymers [ $M$  dependence in Fig. 4(c)]. This result elucidates the  $M$ -independent scaling law for star polymer solutions  $\Pi \propto c^{3\nu/(3\nu-1)}$  in Fig. 2(c). Moreover, because  $c^*$  is an increasing sequence of  $f$  (at fixed  $M$  and  $T$ ), Eq. (6) indicates that  $\Pi$  is a decreasing sequence of  $f$  at fixed  $c$  [ $f$  dependence in Fig. 4(c)]. Therefore, because  $\Pi$  of star polymer solutions follows the universal EOS (1), the  $f$  dependence of  $\Pi$  is originated from the  $f$  dependence of  $c^*$ . Note that the  $f$  dependence of  $c^*$  remains independent of  $M$  [Fig. 4(a)]. Thus, even when  $M$  is sufficiently large and the central core proportion (branching points) to the arms becomes infinitely small, the branching effect on osmotic pressure remains [red characters in Fig. 4(c)].

*Concluding remarks.*— We experimentally measured



$\Pi$  of star polymers with up to eight arms in good solvents near and above the  $c^*$  regime. We found that the universal EOS given in Eq. (1) (Fig. 1) describes  $\Pi$  of these systems, with decreasing  $\Pi$  [Fig. 2(b)] and increasing  $c^*$  [Fig. 2(d)] as the arm number  $f$  increased. We ensured the universality of Eq. (1) (i.e., the function  $f_{\Pi}$ ) for various polymers and solvents, by showing that the scaling relations  $R_g \propto M^\nu$ ,  $\Psi^* \propto M^0$ , and  $c^* \propto M^{1-3\nu}$  were the same as those for the linear polymer solutions [Figs. 3(b), 4(b), and 4(a)]. We also showed that  $R_g$ ,  $\Psi^*$ , and  $c^*$  are decreasing, increasing, and increasing sequences of  $f$ , respectively. The scaling relation  $c^* \propto M^{1-3\nu}$  demonstrates the universality of EOS in star polymer solutions to be consistent with increasing  $M$  and  $f$ , indicating that the  $f$  dependence of  $\Pi$  remains even when  $M \rightarrow \infty$  in the semidilute regime [Fig. 4(c)].

Our findings are beneficial for controlling osmotic pressure in the biomedical and pharmaceutical applications of star polymers [2], such as drug delivery, gene deliv-

ery, surface modifiers, tissue engineering, and medical devices. The universality of EOS in star polymer solutions can further provide an accurate determination of the osmotic pressure of branched polymers [26], including dendrimers [63] and polymer gels [4].

## ACKNOWLEDGMENTS

This work was supported by the Japan Society for the Promotion of Science (JSPS) through the Grants-in-Aid for JSPS Research Fellows Grant No. 202214177 to T.Y., Scientific Research (B) Grant No. 22H01187 to N.S., Early Career Scientists Grant No. 19K14672 to N.S., Scientific Research (A) Grant No. 21H04688 to T.S., Transformative Research Area Grant No. 20H05733 to T.S., and MEXT Program Grant No. JPMXP1122714694 to T.S. This work was also supported by JST through CREST Grant No. JPMJCR1992 and Moon-shot R&D Grant No. 1125941 to T.S.

- 
- [1] M. Daoud, and J. P. Cotton, Star shaped polymers: a model for the conformation and its concentration dependence, *J. Phys.* **43**, 531 (1982).
- [2] W. Wu, W. Wang, and J. Li, Star polymers: Advances in biomedical applications, *Prog. Polym. Sci.* **46**, 55 (2015).
- [3] J. M. Ren, T. G. McKenzie, Q. Fu, E. H. H. Wong, J. Xu, Z. An, S. Shanmugam, T. P. Davis, C. Boyer, and G. G. Qiao, Star polymers, *Chem. Rev.* **116**, 6743 (2016).
- [4] S. Nakagawa and N. Yoshie, Star polymer networks: a toolbox for cross-linked polymers with controlled structure, *Polym. Chem.* **13**, 2074 (2022).
- [5] T. Sakai, T. Matsunaga, Y. Yamamoto, C. Ito, R. Yoshida, S. Suzuki, N. Sasaki, M. Shibayama, and U. Chung, Design and fabrication of a high-strength hydrogel with ideally homogeneous network structure from tetrahedron-like macromonomers, *Macromolecules* **41**, 5379 (2008).
- [6] X. Li, S. Nakagawa, Y. Tsuji, N. Watanabe, and M. Shibayama, Polymer gel with a flexible and highly ordered three-dimensional network synthesized via bond percolation, *Sci. Adv.* **5**, eaax8647 (2019).
- [7] X. Huang, S. Nakagawa, X. Li, M. Shibayama, and N. Yoshie, A simple and versatile method for the construction of nearly ideal polymer networks, *Angew. Chem. Int. Ed.* **59**, 9646 (2020).
- [8] T. Fujiyabu, N. Sakumichi, T. Katashima, C. Liu, K. Mayumi, U. Chung, and T. Sakai, Tri-branched gels: Rubbery materials with the lowest branching factor approach the ideal elastic limit, *Sci. Adv.* **8**, eabk0010 (2022).
- [9] S. C. Grindy, R. Learsch, D. Mozhdzhi, J. Cheng, D. G. Barrett, Z. Guan, and P. B. Messersmith, and N. Holten-Andersen, Control of hierarchical polymer mechanics with bioinspired metal-coordination dynamics, *Nat. Mater.* **14**, 1210 (2015).
- [10] V. Yesilyurt, A. M. Ayob, E. A. Appel, J. T. Borenstein, R. Langer, and D. G. Anderson, Mixed reversible covalent crosslink kinetics enable precise, hierarchical mechanical tuning of hydrogel networks, *Adv. Mater.* **29**, 1605947 (2017).
- [11] B. Marco-Dufort, R. Iten, and M. W. Tibbitt, Linking molecular behavior to macroscopic properties in ideal dynamic covalent networks, *J. Am. Chem. Soc.* **142**, 15371 (2020).
- [12] M. Ahmadi and S. Seiffert, Coordination geometry preference regulates the structure and dynamics of metallo-supramolecular polymer networks, *Macromolecules* **54**, 1388 (2021).
- [13] H. Chen, J. Zhang, W. Yu, Y. Cao, Z. Cao, and Y. Tan, Control Viscoelasticity of Polymer Networks with Crosslinks of Superposed Fast and Slow Dynamics, *Angew. Chem. Int. Ed.* **60**, 22332 (2021).
- [14] M. Ohira, T. Katashima, M. Naito, D. Aoki, Y. Yoshikawa, H. Iwase, S. Takata, K. Miyata, U. Chung, T. Sakai, M. Shibayama, and X. Li, Star-Polymer–DNA Gels Showing Highly Predictable and Tunable Mechanical Responses, *Adv. Mater.* **34**, 2108818 (2022).
- [15] M. Zhong, R. Wang, K. Kawamoto, B. D. Olsen, and J. A. Johnson, Quantifying the impact of molecular defects on polymer network elasticity, *Science* **353**, 1264 (2016).
- [16] S. Seiffert, Origin of nanostructural inhomogeneity in polymer-network gels, *Polym. Chem.* **8**, 4472 (2017).
- [17] Y. Yoshikawa, N. Sakumichi, U. I. Chung, and T. Sakai, Negative Energy Elasticity in a Rubberlike Gel, *Phys. Rev. X* **11**, 011045 (2021).
- [18] T. Fujiyabu, T. Sakai, R. Kudo, Y. Yoshikawa, T. Katashima, U. Chung, and N. Sakumichi, Temperature dependence of polymer network diffusion, *Phys. Rev. Lett.* **127**, 237801 (2021).
- [19] N. Sakumichi, Y. Yoshikawa, and T. Sakai, Linear elasticity of polymer gels in terms of negative energy elasticity, *Polym. J.* **53**, 1293 (2021).

- [20] N. Sakumichi, T. Yasuda, and T. Sakai, Semidilute Principle for Gels, arXiv:2210.15275.
- [21] Y. Higo, N. Ueno, and I. Noda, Osmotic pressure of semidilute solutions of branched polymers, *Polym. J.* **15**, 367 (1983).
- [22] B. J. Cherayil, M. G. Bawendi, A. Miyake, and K. F. Freed, Osmotic pressure of star and ring polymers in semidilute solution, *Macromolecules* **19**, 2770 (1986).
- [23] M. Adam, L. J. Fetters, W. W. Graessley, and T. A. Witten, Concentration dependence of static and dynamic properties for polymeric stars in a good solvent, *Macromolecules* **24**, 2434 (1991).
- [24] G. Merkle, W. Burchard, P. Lutz, K. F. Freed, and J. Gao, Osmotic pressure of linear, star, and ring polymers in semidilute solution. A comparison between experiment and theory, *Macromolecules* **26**, 2736 (1993).
- [25] J. Roovers, P. M. Toporowski, and J. Douglas, Thermodynamic properties of dilute and semidilute solutions of regular star polymers, *Macromolecules* **28**, 7064 (1995).
- [26] W. Burchard, Solution properties of branched macromolecules, *Adv. Polym. Sci.* **143**, 113 (1999).
- [27] G. S. Grest, K. Kremer, and T. A. Witten, Structure of many arm star polymers: a molecular dynamics simulation, *Macromolecules* **20**, 1376 (1987).
- [28] K. Ohno, K. Shida, M. Kimura, and Y. Kawazoe, Monte Carlo study of the second virial coefficient of star polymers in a good solvent, *Macromolecules* **29**, 2269 (1996).
- [29] A. Di Cecca, and J. J. Freire, Monte Carlo simulation of star polymer systems with the bond fluctuation model, *Macromolecules* **35**, 2851 (2002).
- [30] H. P. Hsu, W. Nadler, and P. Grassberger, Scaling of star polymers with 1- 80 arms, *Macromolecules* **37**, 4658 (2004).
- [31] A. M. Rubio and J. J. Freire, Monte Carlo calculation of second virial coefficients for linear and star chains in a good solvent, *Macromolecules* **29**, 6946 (1996).
- [32] D. Ida and T. Yoshizaki, A Monte Carlo study of the second virial coefficient of semiflexible regular three-arm star polymers, *Polym. J.* **40**, 1074 (2008).
- [33] T. Sato, T. Norisuye, and H. Fujita, Second and third virial coefficients for binary polystyrene mixtures in benzene, *J. Polym. Sci., Part B* **25**, 1 (1987).
- [34] Y. Nakamura, T. Norisuye, and A. Teramoto, Third virial coefficient of polystyrene in benzene, *J. Polym. Sci., Part B* **29**, 153 (1991).
- [35] Y. Miyaki, Y. Einaga, and H. Fujita, Excluded-volume effects in dilute polymer solutions. 7. Very high molecular weight polystyrene in benzene and cyclohexane, *Macromolecules* **11**, 1180 (1978).
- [36] M. Okumoto, Y. Nakamura, T. Norisuye, and A. Teramoto, Excluded-volume effects in star polymer solutions: Four-arm star polystyrene in benzene, *Macromolecules* **31**, 1615 (1998).
- [37] M. Okumoto, Y. Iwamoto, Y. Nakamura, and T. Norisuye, Excluded-volume effects in star polymer solutions. Six-arm star polystyrene in benzene, *Polym. J.* **32**, 422 (2000).
- [38] M. Fukuda, M. Fukutomi, Y. Kato, and T. Hashimoto, Solution properties of high molecular weight polystyrene, *J. Polym. Sci., Polym. Phys. Ed.* **12**, 871 (1974).
- [39] A. Yamamoto, M. Fujii, G. Tanaka, and H. Yamakawa, More on the analysis of dilute solution data: polystyrenes prepared anionically in tetrahydrofuran, *Polym. J.* **2**, 799 (1971).
- [40] J. F. Douglas, J. Roovers, and K. F. Freed, Characterization of branching architecture through “universal” ratios of polymer solution properties, *Macromolecules* **23**, 4168 (1990).
- [41] J. Roovers, and P. M. Toporowski, Hydrodynamic studies on model branched polystyrenes, *J. Polym. Sci., Polym. Phys. Ed.* **18**, 1907 (1980).
- [42] J. Roovers, Linear viscoelastic properties of polybutadiene. A comparison with molecular theories, *Polym. J.* **18**, 153 (1986).
- [43] K. Huber, W. Burchard, L. J. Fetters, Dynamic light scattering from regular star-branched molecules, *Macromolecules* **17**, 541 (1984).
- [44] N. Khasat, R. W. Pennisi, N. Hadjichristidis, and L. J. Fetters, Dilute solution behavior of 3-arm asymmetric and regular 3- and 12-arm polystyrene stars, *Macromolecules* **21**, 1100 (1988).
- [45] J. E. L. Roovers and S. Bywater, Preparation of six-branched polystyrene. Thermodynamic and hydrodynamic properties of four- and six-branched star polystyrenes, *Macromolecules* **7**, 443 (1974).
- [46] B. J. Bauer, L. J. Fetters, W. W. Graessley, N. Hadjichristidis, and G. F. Quack, Chain dimensions in dilute polymer solutions: A light-scattering and viscometric study of multiarmed polyisoprene stars in good and *theta* solvents, *Macromolecules* **22**, 2337 (1989).
- [47] J. Roovers, N. Hadjichristidis, and L. J. Fetters, Analysis and dilute solution properties of 12- and 18-arm-star polystyrenes, *Macromolecules* **16**, 214 (1983).
- [48] J. des Cloizeaux, The Lagrangian theory of polymer solutions at intermediate concentrations, *J. Phys. (Paris)* **36**, 281 (1975).
- [49] P. G. de Gennes, *Scaling Concepts in Polymer Physics* (Cornell University Press, Ithaca, 1979).
- [50] T. Ohta and Y. Oono, Conformation space renormalization theory of semidilute polymer solutions, *Phys. Lett.* **89A**, 460 (1982).
- [51] T. Ohta and A. Nakanishi, Theory of semi-dilute polymer solutions. I. Static property in a good solvent, *J. Phys. A* **16**, 4155 (1983).
- [52] Y. Oono, Statistical physics of polymer solutions: conformation-space renormalization-group approach, *Adv. Chem. Phys.* **61**, 301 (1985).
- [53] I. Noda, N. Kato, T. Kitano, and M. Nagasawa, Thermodynamic properties of moderately concentrated solutions of linear polymers, *Macromolecules* **14**, 668 (1981).
- [54] J. des Cloizeaux and I. Noda, Osmotic pressure of long polymers in good solvents at moderate concentrations: a comparison between experiments and theory, *Macromolecules* **15**, 1505 (1982).
- [55] I. Noda, Y. Higo, N. Ueno, and T. Fujimoto, Semidilute region for linear polymers in good solvents, *Macromolecules* **17**, 1055 (1984).
- [56] P. J. Flory, *Principles of Polymer Chemistry* (Cornell University Press, Ithaca, 1953).
- [57] W. H. Stockmayer and E. F. Casassa, The third virial coefficient in polymer solutions, *J. Chem. Phys.* **20**, 1560 (1952).
- [58] A. Pelissetto and E. Vicari, Critical phenomena and renormalization-group theory. *Phys. Rep.* **368**, 549 (2002).
- [59] T. Yasuda, N. Sakumichi, U. I. Chung, and T. Sakai, Universal Equation of State Describes Osmotic Pressure throughout Gelation Process, *Phys. Rev. Lett* **125**,

- 267801 (2020).
- [60] H. Vink, Precision measurements of osmotic pressure in concentrated polymer solutions, *Eur. Polym. J.* **7**, 1411 (1971).
  - [61] S. Kawaguchi, G. Imai, J. Suzuki, A. Miyahara, T. Kitano, and K. Ito, Aqueous solution properties of oligo- and poly(ethylene oxide) by static light scattering and intrinsic viscosity, *Polymer* **38**, 2885 (1997).
  - [62] H. Yamakawa, *Modern Theory of Polymer Solutions* (Harper and Row, New York, 1971).
  - [63] E. Abbasi, S. F. Aval, A. Akbarzadeh, M. Milani, H. T. Nasrabadi, S. W. Joo, Y. Hanifehpour, K. Nejati-Koshki, and R. Pashaei-Asl, Dendrimers: synthesis, applications, and properties, *Nanoscale Res. Lett.* **9**, 247 (2014).

# Supplemental Material for: “Universality of Osmotic Equation of State in Star Polymer Solutions”

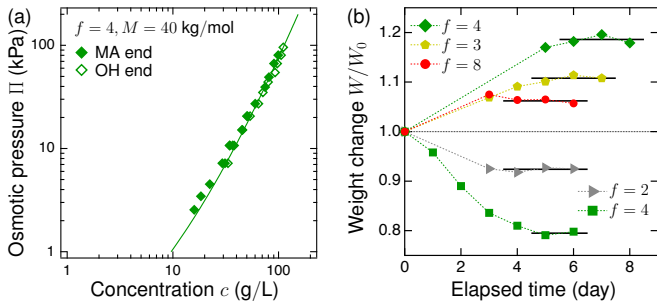


FIG. S1. (a) Polymer mass concentration ( $c$ ) dependence of the osmotic pressure ( $\Pi$ ) in the four-arm star PEG solutions with different functional groups of MA (green-filled diamonds) and OH (green-open diamonds) with  $M = 40$  kg/mol. The data of green-filled diamonds are the same as those in Figs. 1 and 2 in the main text. (b) Time course of the weight-swelling ratio  $W/W_0$  from the as-prepared state ( $W_0$ ) to the equilibrium state ( $W$ ) of PEG solutions in membrane osmometry. For the linear PEG, we set  $c_{\text{ext}} = 60$  g/L for  $c_0 = 40$  g/L with  $M = 20$  kg/mol (gray triangles). For the three-arm star PEG, we set  $c_{\text{ext}} = 55$  g/L for  $c_0 = 30$  g/L with  $M = 20$  kg/mol (yellow pentagons). For the four-arm star PEG, we set  $c_{\text{ext}} = 90$  g/L for  $c_0 = 40$  g/L with  $M = 10$  kg/mol (green squares) and  $c_{\text{ext}} = 80$  g/L for  $c_0 = 60$  g/L with  $M = 40$  kg/mol (green diamonds). For the eight-arm star PEG, we set  $c_{\text{ext}} = 140$  g/L for  $c_0 = 130$  g/L with  $M = 40$  kg/mol (red circles).

## I. EFFECT OF END-FUNCTIONAL GROUPS ON OSMOTIC PRESSURE

We demonstrate that the difference in the end-functional groups is negligible for the osmotic pressure  $\Pi$ . Figure S1(a) shows  $\Pi = \Pi(c)$  for four-arm star polymer (PEG) solutions with maleimide (MA, green-filled diamonds) and hydroxy (OH, green open diamonds) end-functional groups with  $M = 40$  kg/mol. The variation in  $\Pi$  is within experimental accuracy.

## II. VERIFICATION OF REACHING EQUILIBRIUM

To ensure that each solution sample reached equilibrium in membrane osmometry, we show the time course of the weight-swelling ratio  $W/W_0$  for the linear, three-arm, four-arm, and eight-arm star polymer (PEG) solutions in Fig. S1(b). Approximately one week was required to achieve an equilibrium state (horizontal black lines). Thus, we determined the equilibrium state as the point at which  $W/W_0$  remained constant for two to three days.

TABLE S1. Data of the osmotic pressure ( $\Pi$ ) for linear, three-arm, four-arm, and eight-arm star poly(ethylene glycol) in aqueous solutions at 298 K measured in this study.

$c$ (kg/m <sup>3</sup> )	$\Pi$ (kPa)	$c$ (kg/m <sup>3</sup> )	$\Pi$ (kPa)	$c$ (kg/m <sup>3</sup> )	$\Pi$ (kPa)
<b>Linear with <math>M = 20</math> kg/mol</b>					
16.4	3.45	45.3	27.18	73.3	66.70
18.4	4.51	54.0	34.98	82.8	80.38
20.0	5.76	55.5	34.98	83.3	54.64
22.6	7.20	57.8	44.10	83.6	80.38
30.7	10.71	58.2	44.10	95.9	95.74
37.9	15.15	69.7	66.70	97.5	112.99
39.2	15.15	70.3	54.64	99.9	95.74
43.6	20.60	72.1	54.64	109.2	112.99
<b>Three-arm with <math>M = 20</math> kg/mol</b>					
19.7	5.76	45.3	20.60	76.7	54.64
24.3	7.20	45.8	20.60	86.2	66.70
27.0	8.85	56.2	27.18	90.1	80.38
33.4	12.81	69.2	34.98	96.5	95.77
40.2	15.15	73.7	44.10		
<b>Four-arm with <math>M = 10</math> kg/mol (Ref. [59])</b>					
19.7	7.20	43.5	23.75	83.5	66.70
25.5	8.85	50.2	27.18	88.6	66.70
25.8	10.71	50.8	27.18	96.8	80.38
26.9	10.71	56.6	34.98	98.3	80.38
28.5	12.81	58.5	34.98	102.7	95.77
31.4	15.15	63.8	44.10	107.4	95.77
36.0	15.15	64.3	44.10	108.6	95.77
37.4	17.74	75.0	54.64	121.4	112.99
40.1	20.60	76.0	54.64		
<b>Four-arm with <math>M = 40</math> kg/mol (Ref. [59])</b>					
15.9	2.55	34.6	10.71	60.1	27.18
18.4	3.45	37.9	10.71	74.5	39.37
22.3	4.51	45.0	15.15	81.0	49.18
29.3	7.20	45.5	15.15	90.4	60.70
31.1	7.20	50.1	20.60	99.1	80.38
34.3	10.71	50.7	20.60		
<b>Eight-arm with <math>M = 40</math> kg/mol</b>					
18.0	2.55	49.4	10.71	109.2	66.70
20.2	3.45	52.1	15.15	109.9	66.70
22.8	4.51	55.8	17.74	111.2	54.64
29.4	4.51	72.4	20.60	117.0	80.38
30.1	4.51	77.1	27.18	121.1	80.38
33.3	7.20	79.5	27.18	122.3	66.70
35.2	7.20	81.0	27.18	123.4	95.77
35.8	7.20	82.8	34.98	123.6	95.77
36.9	4.51	97.1	34.98	125.7	80.38
42.8	10.71	100.9	44.99	137.2	113.00
43.3	7.20	103.7	54.64	157.0	113.00
46.2	12.81	105.7	44.99		
46.2	12.81	106.3	66.70		



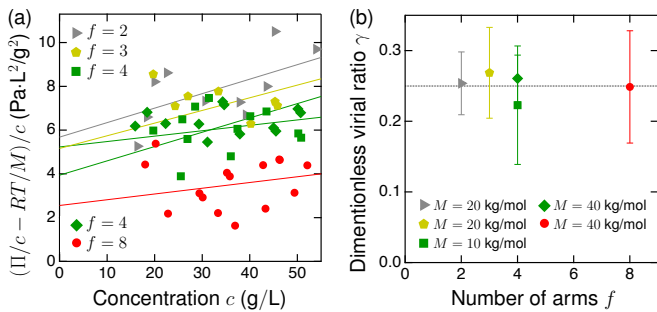


FIG. S2. (a) Evaluation of the dimensionless virial ratio  $\gamma$ . Each solid line is obtained from the one-parameter least-square fit of  $\gamma$  with Eq. (S1) to the data for each sample, using  $c^*$  estimated in Fig. 2(d) in the main text. According to Eq. (S1), the slope of each best fit line gives  $\gamma$  of each arm number  $f$ . (b) Dimensionless virial ratio  $\gamma$  for various  $f$ . The error bar indicates the standard error of the least-square fit. The dashed line represents  $\gamma \approx 0.25$  for the linear polymer solutions [56].

### III. DATA OF OSMOTIC PRESSURE OF LINEAR AND STAR PEG IN AQUEOUS SOLUTIONS

All experimental data of the osmotic pressure  $\Pi$  at various polymer mass concentrations  $c$  measured via membrane osmometry in this study are listed in Table. S1.

### IV. THIRD VIRIAL COEFFICIENT OF STAR POLYMER SOLUTIONS

We evaluated the third virial coefficient in linear and star polymer (PEG) solutions based on the concentration ( $c$ ) dependence of osmotic pressure  $\Pi$ . In the universal EOS given by Eq. (1) in the main text, the third virial coefficient  $A_3$  corresponds to the dimensionless virial ratio  $\gamma \equiv A_3/(A_2^2 M)$  defined in Eq. (2) in the main text. From the virial expansion up to the third order [Eq. (2) in the main text], we have

$$\left(\frac{\Pi}{c} - \frac{RT}{M}\right) \frac{1}{c} = \frac{RT}{Mc^*} \left(1 + \frac{c\gamma}{c^*}\right). \quad (\text{S1})$$

Using  $M$  for each sample and  $c^*$  evaluated in Fig. 2(d) in the main text at 298 K, we show that the one-parameter least-squares fit to the data of  $c$  dependence of  $(\Pi/c - RT/M)/c$  in Fig. S2(a). The slopes of the best-fit lines in Fig. S2(a) give  $\gamma$  for each sample.

For the linear, three-arm, four-arm, and eight-arm star polymer solutions, we have  $\gamma = 0.25(4)$ ,  $\gamma = 0.27(6)$ ,  $\gamma = 0.20(8)$  (with  $M = 10$  kg/mol) and  $\gamma = 0.26(3)$  (with  $M = 40$  kg/mol), and  $\gamma = 0.25(8)$ , respectively.

Numbers in parentheses represent standard errors. For the linear polymer solutions, the obtained  $\gamma$  is consistent with  $\gamma \approx 0.25$  [56]. Although the error bounds are not small for the three-, four-, and eight-arm star polymer solutions, the obtained  $\gamma$  agrees well with  $\gamma \approx 0.25$  for linear polymer solutions [56]. This result is consistent with the result that star polymer solutions with up to eight arms are described by the universal EOS (Fig. 1 in the main text).

### V. PREVIOUS RESEARCH FOR DILUTE LINEAR AND STAR POLYMERS IN GOOD SOLVENT

In Figs. 3(b) and 4(a) and (b) in the main text, we exhibit the dilute solution properties of  $R_g$ ,  $A_2$ , and  $\Psi^*$  with various  $M$ ,  $T$ , and types of polymer and solvent for linear and star polymers in good solvents. All the data were measured through the light scattering reported in Refs. [33–47].

For Figs. 2(b) and 3(a) in the main text, we used the linear (black upward triangles [33–35]), four-arm (green rightward triangles [36]), and six-arm (blue downward triangles [37]) poly(styrene) (PS) in benzene (Bz) at 298 K.

For the main panel and the inset in Fig. 3(b) in the main text, we used data from linear PS in Bz at 298 K (upward triangles [33–35]), linear PS in Bz at 303 K (lower left triangles [38] and upper left triangles [39]), linear PS in toluene (TL) at 303 K (black upper left triangles [39]), linear PS in TL at 308 K (squares [40, 41]), linear poly(butadiene) (PB) in cyclohexane (CH) at 308 K (squares [40, 42]), three-arm star PS in TL at 293 K (lower-right triangles, [43]), three-arm star PS in TL at 308 K (upper-right triangles, [44]), four-arm star PS in Bz at 298 K (rightward triangles [36]), four-arm star PB in CH at 298 K (squares [40]), six-arm star PS in Bz at 298 K (downward triangles [37]), six-arm star PB in CH at 298 K (squares [40, 45]), eight-arm star poly(isoprene) (PI) in CH at 296 K (diamonds [46]), ten-arm star PI in CH at 296 K (diamonds [46]), twelve-arm star PI in CH at 296 K (diamonds [46]), twelve-arm star PS in TL at 308 K (leftward triangles [47]), eighteen-arm star PB in CH at 298 K (squares [40]), eighteen-arm star PI in CH at 296 K (diamonds [46]), eighteen-arm star PS in TL at 298 K (leftward triangles [47]), twenty-two arm star PI in CH at 296 K (diamonds [46]), twenty-six arm star PI in CH at 296 K (diamonds [46]), thirty-two arm star PI in CH at 296 K (diamonds [46]), and fifty-six arm star PI in CH at 296 K (diamonds [46]).